04

Cathode erosion in a gas arc discharge at the threshold currents

© A.M. Murzakaev

Institute of Electrophysics, Ural Branch, Russian Academy of Sciences,
620016 Yekaterinburg, Russia
e-mail: Amurzak@mail.ru

Received April 20, 2021
Revised June 16, 2021
Accepted June 17, 2021

The results of experimental studies of the erosion rate of high-purity tungsten cathodes after pulsed arc discharges in a pure oil-free ultrahigh vacuum and in gases of various purities are reported. The erosion rate in high-purity argon does not change compared to the rate of erosion of electrodes in a pure oil-free vacuum. The rate of erosion in „technical" argon is 10−20% less than the rate of erosion of electrodes in an oil-free vacuum. The rate of erosion in „technical" nitrogen is 15−35% less than the rate of erosion of electrodes in vacuum. Particle sizes formed in gas arcs are smaller than those formed in vacuum arcs.

Keywords: arc in gas, erosion rate, ecton mechanism, particles, electron microscopy

DOI: 10.21883/TP.2022.14.55217.114-21

Introduction

An electric arc in an inert gas with a tungsten pointed cathode and a cooled anode has found wide application in industry. A general idea of gas arcs can be found in [1]. With cold cathodes, both gas and vacuum arcs have many common characteristics, for example, the arc discharge burning is approximately the same in vacuum and in gas with a wide range of pressure changes of the surrounding gas. Therefore, it seemed plausible that the main physical processes in the cathode spot (CS), such as plasma formation from the cathode material, evaporation of the cathode material and current transfer in the interelectrode space, remain unchanged when gas is added to the discharge chamber. In [2,3], a decrease in specific erosion by an order of magnitude in gas arcs compared to vacuum arcs [4,5] was revealed. For vacuum arcs, it was found that cathode erosion consists of three components: ions, neutral vapors, and droplets ranging in size from 0.1 to 10 μm [6–9]. Drops at first glance are more a by-product than an active component of the CS, since they do not affect the electrical characteristics. The ionic current ranges from 6 to 10% of the total arc current and depends on the cathode material. Vapors are formed at the CS due to the heating of the cathode and due to the evaporation of liquid metal droplets. According to [7,10], the proportion of vapor erosion ranges from a few percent to 10−20% of the total erosion and depends on the cathode material. The dynamics of CS fragments and cells is influenced by the surrounding gas. At some distance from the center of the CS, the expansion of the metal plasma [11–14] becomes difficult. The appearance of new CS beyond the plasma propagation region of the cathode material means that their formation occurs due to the interaction of the gas plasma with the cathode surface.

It is known that in gases reacting with electrodes, the surfaces of the electrodes are covered with polluting layers. In the air, the surface of the electrodes is covered with [15] oxides. In [16], nitrogen films with a thickness of 10 nm at a pressure of 670 Pa and a thickness twice as large at a pressure of 1300 Pa were found. In [15,17,18], the influence of pollution layers on the types of spots and their movement was studied. It was found that with an increase in gas pressure, spots of the first type begin to prevail, i.e. surface contamination contributes to the ignition of new CS at large distances from the existing one.

It follows from the analysis of these studies that the erosion of electrodes in vacuum and gases is strongly influenced by the surface condition (cleanliness) of the electrodes. Due to poorly defined electrode surface conditions, a wide variety of results is difficult to interpret. These contradictory data on the values of specific erosion require more thorough experimental verification.

1. Material and experimental procedure

All the experiments were carried out in the same stainless steel chamber equipped with an observation window. The block diagram of the experiments is shown in Figure 1. In all series of experiments, the cathode, anode and igniting electrode materials were made of tungsten wire with a diameter of 0.1mm and a purity of 99.98%. Wire electrodes were prepared according to the following procedure: to remove graphite (carbon) from the surface of the wire after drawing and leveling the surface, the wire was electrochemically polished, washed with distilled water and ethyl alcohol. The vacuum was obtained by pumping by oil-free techniques — a zeolite pre-vacuum pump when cooled with liquid nitrogen and an ionization magnetic discharge pump. With constant pumping, the electrodes were cleaned by heating by passing current through them

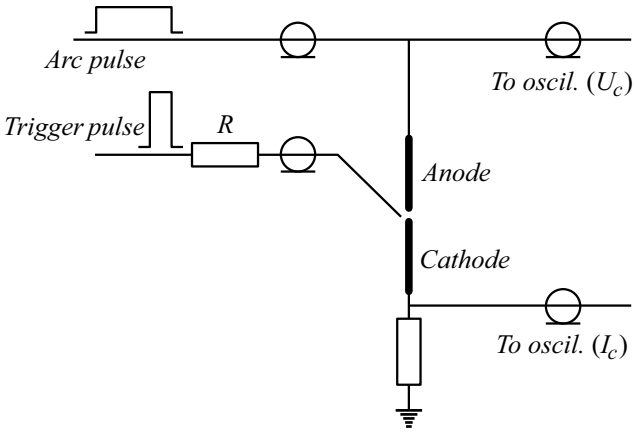

Figure 1. Diagram of the experiment.

at a temperature just below the melting point. The technique of heating the electrodes is described in detail in [19]. According to the nomogram for calculating tungsten wire cathodes and heaters with a known wire diameter and length, the current value for heating the wire to the required temperature was obtained. In the first series of experiments, the temperature of the electrodes was measured with a pyrometer. The results obtained were practically the same. When conducting experiments to determine the specific erosion of electrodes during a gas arc discharge, the vacuum pump was cut off. The experimental chamber was constantly filled with gas to a pressure slightly above atmospheric pressure through a stainless steel needle nozzle. The gas was constantly updated with a flow rate of 0.1 l/min. The gases used had the following characteristics: nitrogen by GOST 9293-74, nitrogen content not less than 99.99%, oxygen content not more than 0.001% by volume; argon by GOST 10157-79, first grade, argon content not less than 99.987%, oxygen content not more than 0.002% volume fraction; high purity argon according to TU 2114-005-0024760-99, argon content not less than 99.998%, oxygen content not more than 0.0002% volume fraction.

The electric arc was powered by a cable generator. The duration of the rectangular arc pulse was $1.2\,\mu$s. In order to avoid increase of the arc discharge power pulse front, the electrical coaxial inputs of the experimental chamber were matched with the wave resistance of the generator $\rho = 75\,\Omega$. The control studies determined the bandwidth of the electrical inputs of the vacuum chamber, and the registration system made it possible to reliably observe voltage drops with a front duration of 0.9 ns. The inductance of the discharge chamber was 10 nH, and it was practically determined by the inductance of the wire electrodes. The arc discharge was ignited by a tip ignition electrode (the tip diameter is less than $5\,\mu$m) located at a distance of 10 to $50\,\mu$m from the top of the cathode, and a pulsed positive voltage with an amplitude of 20 kV and a duration of 20 was applied to the tip,ns. The current of the igniting pulse was limited to 2 A by means of a resistor R connected to the circuit of the igniting pulse. The arc discharge current was 10 A and was measured using calibrated resistive shunts. The magnitude and duration of the arc discharge current pulse were known for each pulse from the waveforms obtained by oscilloscopes with a bandwidth of 10 GHz. The effect of the igniting current pulse on the total specific erosion is negligible, since the ignition current is 5 times less than the arc current and the duration of the ignition current is 60 times less than the arc burning time.

During the arc burning process, the electrodes were visually monitored using an optical microscope. By photographing the cathode tip in an optical microscope before and after a series of arc discharge combustion pulses, the shortening of the wire cathode was determined and its mass loss was estimated. Electrode surfaces and particles were studied with scanning electron microscopes (SEM) JSM-T220 and LEO 982. The transmission electron microscope (TEM) JEM-2100 was used for the analysis of nanoscale particles.

2. Experimental results and discussion

After the experiments, no traces of the existence of anode spots were observed on the surface of the anodes and igniting electrodes, and no drops of cathode material were detected due to the transfer of material from the cathode to the anode or to the igniting electrode. Anodes and igniting electrodes did not contribute to cathode erosion. It should be particularly noted that the specific erosion of the cathode under pure vacuum conditions in a vacuum arc in our experimental conditions for a tungsten cathode was $(2-4)\cdot 10^{-4}$ g/C. With an increase in the pressure of high-purity argon from 10^{-6} to 10^{5} Pa in a low-current arc, there is no change in the erosion rate compared to the specific erosion in a vacuum arc discharge under pure vacuum conditions. During the arc discharge burning in the atmosphere of argon technical purity, the erosion rate decreased to 10% compared to the erosion rate during vacuum arc discharge. This decrease in the magnitude of specific erosion can only be caused by the formation of films of contamination on the cathode surface when a gas with a higher oxygen content is introduced into the experimental chamber. The specific erosion during the arc discharge in the nitrogen atmosphere decreased from 15 to 35% compared to the specific erosion during vacuum arc discharge. The oxygen content in nitrogen is lower compared to argon of technical purity. Therefore, such a decrease in the magnitude of specific erosion can be caused not only by the influence of oxygen, but also by the formation of „contamination“ on the cathode surface when nitrogen is introduced into the experimental chamber.

These results provide strong grounds for the assumption that surface contamination plays an important role in creating conditions responsible for reducing the current

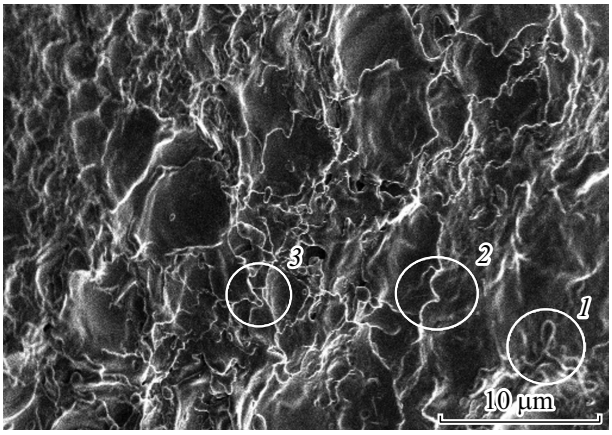

Figure 2. The cathode surface with frozen craters and jets of liquid metal.

carried by the CS and reducing the rate of erosion. It can be assumed that a separate CS operating at a given current level in a high purity gas has many of the same basic characteristics as a separate CS operating at such a current level in a vacuum.

In the process of determining specific erosion, the drip component of erosion was also studied. Droplets are formed due to the spraying of liquid metal from the cathode surface due to the reactive pressure of the CS plasma. Part of this liquid metal remains on the cathode surface in the form of frozen jets, which are visible in Figure 2 (marked with circles). Almost all the drops flew to the side surface. In vacuum, droplets are reflected from the walls of the experimental chamber several times before settling on the surface of the experimental chamber or on a specially installed screen. Large drops in the process of impact disintegrated into smaller ones. Some of the large droplets that stuck to the surface of the screen are deformed upon impact and have a flat shape, as can be seen in Figure 3. This indicates that these droplets were still in the liquid phase when they hit the screen surface and only after that they solidified. However, not all drops are deformed. Particles smaller than $0.5\,\mu$m — are spherical, which indicates that they either cooled down and solidified before impact in flight, or after impact and sticking of still liquid droplets, surface tension forces returned them to their original spherical shape and only after that the droplets solidified. Prior to this, many studies reported that the lower limit of the droplet size was about $0.1\,\mu$m. This lower limit of the droplet size is probably related to the spatial resolution of the imaging device (scanning electron microscope or scanning tunneling microscope), and not to a physically significant limit, and it was not clear a priori whether there is a lower limit of the droplet particle size. In fact, Figure 3 shows the presence of particles on the surface of the collector and on the surface of large particles smaller than 10 nm.

In gas arcs, particles due to deceleration in the gas and a decrease in their flight speed are reflected significantly less from the walls of the experimental chamber compared to vacuum arc discharge. Almost all the particles are — spherical, and this indicates that they were liquid and cooled down, retaining their shape. The characteristic pattern of particles after an arc discharge in argon is shown in Figure 4. The largest drops were smaller than $3\,\mu$m. The characteristic pattern of particles after an arc discharge in nitrogen is shown in Figure 5. For analysis, smaller particles were collected on a carbon film placed on a copper mesh for a transmission electron microscope. Despite the fact that large droplets tore and pierced this carbon film, it was possible to collect the necessary material for analysis. Figure 6 shows atypical photo of nanoparticles. The average particle size is about 60 nm and particles of size 6–7 nm are visible. As a rule, the shape of the particle is close to spherical. The study of the granulometric composition showed that the nanoparticles have a lognormal distribution, the average geometric particle size was $d_g = 57$ nm. A high-resolution TEM picture of tungsten nanoparticles is shown in Figure 7, *a*. After processing the picture — obtaining a fast Fourier transform, applying a circular mask to the Fourier transform and inversion — we get a picture of a nanoparticle with an oxide shell (Figure 7, *b*).

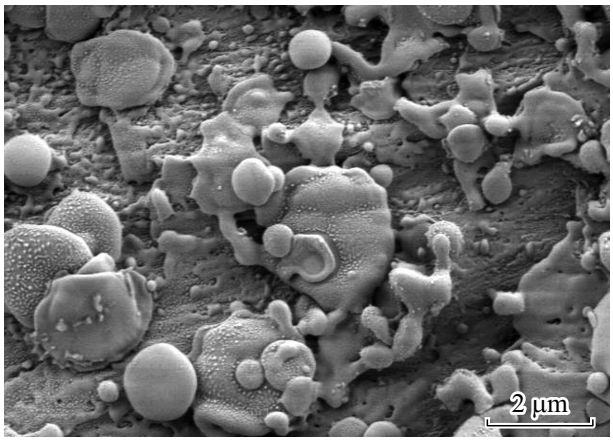

Figure 3. SEM picture of particles after vacuum arc discharge.

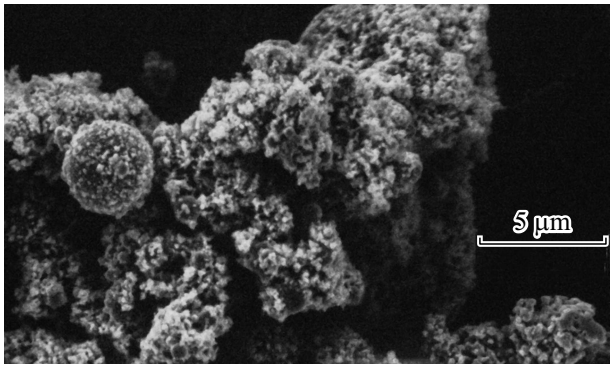

Figure 4. SEM picture of particles after arc discharge in argon.

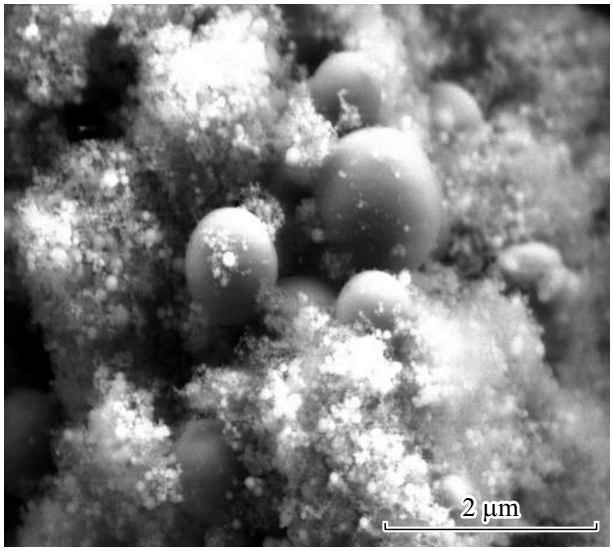

Figure 5. SEM picture of particles after arc discharge in nitrogen.

The main distinguishing feature of a gas arc, unlike a vacuum arc, is the formation of a large number of particles in the nanometer range. This result can be explained as follows. Near the CS, vapor begins to condense with the formation of nanoparticles, then most of the vapors, expanding in vacuum, flies freely, settles on the walls of the experimental chamber or on a specially installed screen and forms a film. When an arc discharge is burning in a gas, the vapor from the cathode material is inhibited by the surrounding gas. In an inert gas, most of the metal vapors condense during cooling and forms nanoparticles. In a gas containing oxygen, in addition to condensation processes, oxidation (burning) occurs, and in nitrogen, the formation of nitrides is possible. Therefore, when an arc discharge is functioning in a gas, the number of particles in the nanometer range is greater.

The concept of similarity of the CS mechanisms of vacuum and gas arcs is quite likely. The magnitude of the specific erosion of the cathode of an arc discharge in an oil-free vacuum and an arc discharge in high-purity argon do not differ. Significant differences in the results of earlier experiments in the rates of arc erosion in vacuum and gas arcs can be explained by the influence of „active“ surface contamination. There are issues that require understanding the role of the contaminating film. The films can have a thickness of only a few tenths of a nanometer, and they quickly break down at high CS temperatures. But, despite this, they play an important role in reducing the average current per spot at high pressures with a corresponding decrease in specific erosion. One of the possible effects of surface contaminants is that they change the surface operation of the output and that the output operation may be one of the factors affecting the average CS current. This is confirmed by the fact that the adsorbed gas changes the output operation in auto-emission observations.

In connection with the developing ectonic arc concept [20] the role of liquid metal droplets and jets in the mechanism of CS functioning is changing significantly. In the study [21], erosive structures on the surface of a tungsten cathode formed during a single burning of a vacuum arc with a current from 4 to 20 A and a duration of up to 700 ns were investigated. It was found that the average mass of frozen micron-sized protrusions on the cathode surface is equal to the mass of ions removed from the cathode during the combustion of the CS cell. The formation time of a new liquid-metal jet under the action of the reactive force of the CS plasma is about 10 ns, which is comparable to the lifetime of the CS. The growth rate of a liquid metal jet is of the order of 10^2 m/s. The geometric shape and size of the solidified jet are such that a new explosive emission center can be formed within a few nanoseconds when the jet interacts with a dense cathode plasma. This is the main self-sustaining mechanism of the vacuum arc.

In this regard, the erosive structures on the cathode surface formed as a result of the action of the CS arc in pure argon were carefully considered (Figure 2). Despite repeated arc discharges and superimposition of erosion traces on each other, the erosion traces of the CS contain a large number of frozen protrusions. They do not differ from the erosion traces of a vacuum arc. In Figure 2 (in circles *1–3*) you can see frozen jets and not separated drops. This suggests that the micron-sized jets at the final stage of their development were liquid metal protrusions. Estimated by the technique described in [20], the average mass of micro-steps (frozen jets) on the cathode surface is equal in order of magnitude to the mass of ions removed from the cathode during one cycle of combustion of the CS cell with a current of 10 A at one place.

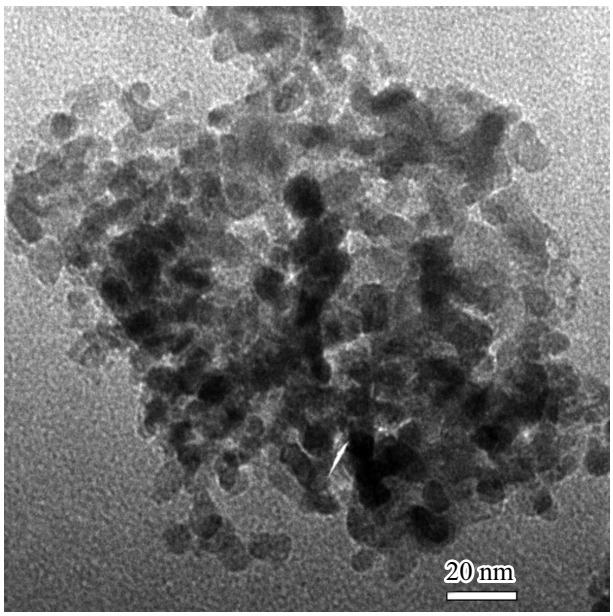

Figure 6. TEM picture of nanoparticles after gas arc discharge.

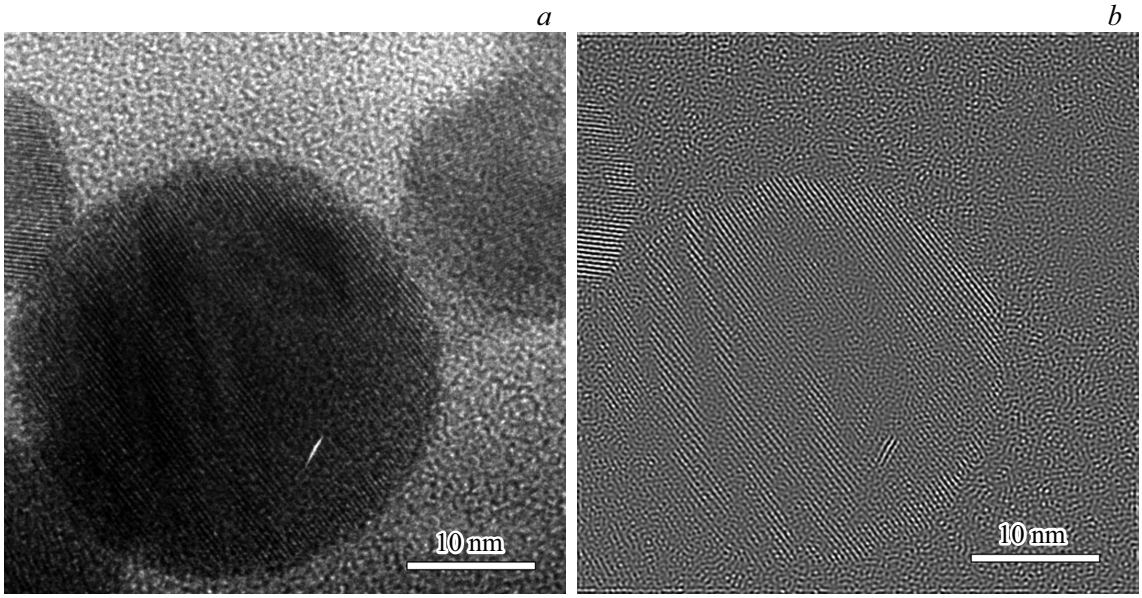

Figure 7. TEM is a high-resolution picture of tungsten nanoparticles (*a*) and a picture of an oxide-coated nanoparticle obtained after processing (*b*).

In [22], a hydrodynamic analysis of the behavior of a „puddle“ of liquid metal in the CS region allowed us to estimate the threshold values of plasma pressure and electric current flowing through the crater, at which liquid metal begins to splash out in the form of jets and droplets. It has been shown that a crater can be formed by extrusion of liquid metal by plasma in 30 ns if the heat flux density is higher 10^{12} W/m^2 and the pressure is higher 10^8 Pa. This amount of pressure is comparable to the pressure at the bottom of the Mariana Trench. Therefore, the external gas pressure in the experimental setup should have a weak (insignificant) effect on the physical processes in the CS.

Conclusion

The results of the research showed that the value of specific erosion of tungsten cathodes in an arc discharge in a high-purity argon atmosphere does not change in comparison with the value of specific erosion in an arc discharge in an oil-free vacuum. An increase in the oxygen content even by one thousandth of a percent in argon helps to reduce the specific erosion to 10%. The specific erosion of the cathode in nitrogen arcs is less than the specific erosion in vacuum arcs. We believe that the surface pollution introduced by gas plays an important role in creating conditions responsible for reducing the current carried by one CS, and this leads to a decrease in specific erosion. The particle size after gas arcs is smaller than the particle size after vacuum arcs. The size of nanoparticles in nitrogen arcs is smaller than the size of nanoparticles in argon arcs. The formation of nanoparticles in a gas arc is greater than in a vacuum arc.

The erosive structures on the cathode surface (craters, frozen jets and not separated drops) formed as a result of the action of the CS arc in pure argon do not differ from the erosive structures of the vacuum arc. It can be stated that the interaction of the CS with liquid metal protrusions on the cathode surface inevitably leads to explosive electron emission. Apparently, droplets, jets and plasma also provide the process of self-maintenance of the gas arc.

We assume that a separate CS operating at a given current level in high-purity argon has many of the same basic characteristics as a separate CS operating at such a current level in pure vacuum conditions. The concept of similarity of the CS functioning mechanisms of both vacuum arcs and high-pressure arcs seems quite plausible.

Acknowledgments

This study was carried out using the equipment of the Central Research Institute of the IEF of the Ural Branch of the Russian Academy of Sciences.

Funding

This study has been performed under state assignment № AAAA-A18-118030290007-5 and № AAAA-A18-118030290006-8.

Conflict of interest

The author declares that he has no conflict of interest.

References

[1] Yu.P. Rayzer. *Fizika gazovogo razryada* (Nauka, M., 1987) (in Russian).
[2] R.N. Szente, R.J. Munz, M.G. Drouet. Plasma Chem. Plasma Proces., **12** (3), 327 (1992). DOI: 10.1007/bf01447029
[3] J.L. Meunier, M.G. Drouet. IEEE Trans. Plasma Sci., **15** (5), 515 (1987). DOI: 10.1109/tps.1987.4316746
[4] C.W. Kimblin. J. Appl. Phys., **44**, 3074 (1973). DOI: 10.1063/1.1662710
[5] C.W. Kimblin. J. Appl. Phys. **45**, 5235 (1974). DOI: 10.1063/1.16632222
[6] J.E. Daalder. J. Phys. D: Appl. Phys., **8**, 1647 (1975). DOI: 10.1088/0022-3727/8/14/009
[7] J.E. Daalder. J. Phys. D: Appl. Phys., **9**, 2379 (1976). DOI: 10.1088/0022-3727/9/16/009
[8] A. Anders, E.M. Oks, G.Y. Yushkov, K.P. Savkin, I.G. Brown, A.G. Nikolaev. IEEE Transactions on Plasma Sci., **33** (5), 1532 (2005). DOI: 10.1109/tps.2005.856502
[9] S. Anders, A. Anders, R.M. Yu, X.Y. Yao, I.G. Brown. IEEE Trans. Plasma Sci., **21** (5), 440 (1993). DOI: 10.1109/27.249623
[10] W.D. Davis, H.C. Miller. J. Appl. Phys., **40** (5), 2212 (1969).
[14] M.G. Drouet, J.L. Meunier. IEEE Trans. Plasma Sci., **13**, 285 (1985). DOI: 10.1109/TPS.1985.4316421
[12] J.L. Meunier, M.G. Drouet. IEEE Trans. Plasma Sci., **15** (5), 515 (1987). DOI: 10.1109/tps.1987.4316746
[13] J.L. Meunier. IEEE Trans. Plasma Sci., **18** (6), 904 (1990). DOI: 10.1109/27.61501
[14] R.L. Boxman, S. Goldsmith. IEEE Trans. Plasma Sci., **18** (2), 231 (1990). DOI: 10.1109/27.131026
[15] D.R. Porto, C.W. Kimblin, D.T. Tuma. Appl. Phys., **53** (7), 4740 (1982). DOI.org/10.1063/1.331302
[16] S. Anders, B. Juttner. IEEE Trans. Plasma Sci., **19** (5), 705 (1991). DOI: 10.1109/27.108402
[17] B. Juttner. J. Phys., IV, **07** (C4), C4-31 (1997). DOI: 10.1051/jp4:1997404
[18] B. Juttner. J. Phys. D: Appl. Phys., **34**, 103 (2001).
[19] F. Rosebury. *Handbook of Electron Tube and Vacuum Techniques* (Massachusetts, 1964)
[20] G.A. Mesyats. *Ektony v vakuumnom razryade: proboy iskra, duga* (Nauka, M., 2000) (in Russian).
[21] G.A. Mesyats, M.B. Bochkarev, A.A. Petrov, S.A. Barengolts. Appl. Phys. Lett., **104**, 184101 (2014). DOI: 10.1063/1.4874628
[22] G.A. Mesyats, I.V. Uimanov. IEEE Trans. Plasma Sci., **43** (8), 2241 (2015). DOI: 10.1109/TPS.2015.2431317